Progress In Electromagnetics Research B, Vol. 80, 151–171, 2018

Diurnal and Monthly Variations of Rain Rate and Rain Attenuation on Ka-Band Satellite Communication in South Korea

Sujan Shrestha and Dong-You Choi*

Abstract—Statistics of monthly and diurnal variations in the occurrence of rain fades are needed to give a detailed insight for system design of these services. This paper analyses the performance on three years of rain rate and rain attenuation measurement to study the empirical determination of power law coefficients calculated for monthly distribution of rain attenuation from the knowledge of rain rate at 19.8 GHz link for COMS1 in South Korea. The received signal data for rain attenuation and rain rate were collected at 10 second intervals over a three year period from 2013 to 2015. The comparison of measured data for monthly variation illustrates the suitability for the estimation of signal in Ka-band whose appropriateness is verified through the comparison with prominent rain attenuation models namely ITU-R P. 618-12 and empirically generated regression coefficients values for ITU-R P. 838-3. A monthly variation of the coefficients has been indicated, and the empirical measured data were compared with the ITU-R P. 838-3 derived regression coefficients. Moreover, the statistics analyzed to 6 hour contiguous periods of the day are also shown. Furthermore, the paper presents an overview of the predicted monthly variation of rain attenuation estimation of 2013 year for Ka band in 19.8 and 20.73 GHz from 12.25 GHz link which are obtained from the ITU-R P. 618-13 frequency scaling method, and these predictions are compared with experimentally measured values. These statistics can be useful for communication systems whose service quality and design require seasonal and diurnal variation.

1. INTRODUCTION

In recent days, there is growing demand of satellite capacity in order to support the new services which had led to the use of higher frequency band as Ka band (20/30 GHz) that is most susceptible to rain fade [1]. The severity of atmospheric impairments especially due to rain on radio wave propagation increases markedly with the increase in frequency. Therefore, extensive knowledge of propagation phenomena affecting the system availability and signal quality in these bands are required. The study for time varying rain characterization and diurnal variation in the satellite systems have been studied in [2]. The higher frequency bands have been preferable to provide Direct to Home (DTH) multi-media services. In order to optimize the performance of slant path communication system, it is preferential to determine the period of rain fade, time of day for its occurrence and how often these activities happen [3]. Rain attenuation in satellite communication systems operating at Ka-band frequencies is more severe than usually experienced at lower frequency bands [4]. The total attenuation statistics are correlated with the attenuation statistics of the month of the year [5] as well as on the hour of the day [6] which signifies the appropriate fade margin for satellite systems. The variabilities of diurnal and seasonal variation have been taken into account in fade margin design for fixed scheduled services which have to fulfill the requirement in terms of quality of service which can be easily allocated in different time slots during the day [7]. The annual and diurnal attenuation statistics are studied to understand the rain induced attenuation effect and the possibility of using selective time period for better link availability

Received 2 February 2018, Accepted 30 March 2018, Scheduled 27 April 2018
* Corresponding author: Dong-You Choi (dychoi@chosun.ac.kr).
The authors are with the Department of Information and Communications Engineering, Chosun University, Republic of Korea.

in the studied location [8]. A number of mitigation techniques have been envisioned and experimented over the years, in the attempt to overcome the problem and to make Ka-band satellite applications as commercially viable as those at Ku-band [9]. The methods for the prediction of rain attenuation for a given path have been grouped into two categories, namely, physical and semi-empirical approaches. The physical approach considered the path attenuation as an integral of all individual increments of rain attenuation caused by the drops encountered along the path. Unfortunately, rain cannot be described accurately along the path without extensive meteorological database, which does not exist in most regions of the world [10]. In addition, when physical approach is used, all the input parameters needed for the analysis are not readily available [11]. Most prediction models therefore resort to semi-empirical approaches which depend on two factors, namely, rain rate at a point on the surface of the earth and the effective path length over which rain can be considered to be homogeneous [12]. The ITU-R P. 618-12 is considered preferable for its simplicity and reasonable accuracy, at least for frequencies up to approximately 55 GHz [13]. The integration time of 1-minute rain rate is considered preferential statistics for rain attenuation prediction. Further investigation has been performed locally in South Korea, in order to derive the prediction model [14, 15, 28]. In addition, the rain attenuation effects have been analyzed for Koreasat-3 satellite from the database provided by the Yong-in Satellite Control Office where the emphasis has been mentioned for the ITU-R prediction model [16, 17]. Similarly, the rain attenuation effects have been studied for the terrestrial network in [27]. The preliminary bases for estimation of rain attenuation on slant path applicable for Ka-band have been studied with the combined values of rain attenuation for three years in South Korea [18]. The analysis of the results shows that location with greater variability in rainfall amount, which is considered on annual, seasonal, monthly or hourly basis present higher variability in the corresponding annual, seasonal, monthly or hourly statistics [31]. The probable duration of rain fade, the time of day when it is likely to occur, and how frequently it happens are all important aspects for the design of satellite services [32]. The impact on signal availability which is based on seasonal and diurnal variations are described in [33]. The statistical distributions of rainfall rate and total attenuation are computed and compared with ITU-R prediction methods have been studied [34].

This paper presents the technique for predicting the rain attenuation of beacon signal received in 19.8 GHz frequency during rain events at Mokdong-13 na-gil, Yangcheong-gu, Seoul, Republic of Korea which has been analyzed for monthly basis to understand the variation of rain induced attenuation provided by National Radio Research Agency, RRA studied for earth space communication. The diurnal variation has been studied to know the applicable diurnal fades margin level. The techniques in [18] have been further studied which utilize power law relationship between the effective path length and rain rate and predict the attenuation values for other time percentages as per the ITU-R P. 618-13 extrapolation approach. This paper studies the result of measured rain attenuation compared with the cumulative probability distribution of ITU-R P. 618-13 and ITU-R P. 838-3 methods and studies suitable means to characterize the rain attenuation behavior for 19.8 GHz satellite communication links. The rest of this paper is organized as follows. Section 2 shows a brief overview of selected rain attenuation models. Experimental system along with proposed approach is described in Section 3. Based on the pertinent models and experimental setup, Section 4 presents the statistical analysis with particular emphasis on predicted and measured rain attenuation along with the frequency scaling technique adopted to predict attenuation values for 20.73, 19.8 GHz links from 12.25 GHz for same and different path respectively performed for 2013. Finally, conclusions are drawn in Section 5.

2. LITERATURE REVIEW

The specific attenuation is a fundamental quantity in calculation of rain attenuation statistics for earth space paths [20]. Generally, the attenuation prediction model consists of three methodologies, namely, the calculation of specific attenuation [19], the calculation of rain height [21] and the attenuation calculation methodology. The values of k and α depend on the path elevation angle and polarizations of the measured beacons. The total attenuation is determined as,

$$A\,(\text{dB}) = \gamma_R\,(\text{dB/km}) \times L_{eff}\,(\text{km}) \tag{1}$$

where γ_R (dB/km) is the specific attenuation, and L_{eff} (km) is the effective path length. L_{eff} is the length of a hypothetical path obtained from radio data dividing the total attenuation by specific attenuation exceeded for the same percentage of time. The recommendation of the ITU-R P. 838-3 [19] establishes the procedure of specific attenuation from the rain intensity. The specific attenuation γ_R (dB/km) is obtained from the rain rate R (mm/h) exceeded at p percent of the time using the power law relationship as,

$$\gamma_R = kR^{\alpha} \tag{2}$$

where k and α depend on the frequency and polarization of the electromagnetic wave. The constants appear in recommendation tables of ITU-R P. 838-3 [19] and can also be obtained by interpolation considering a logarithmic scale for k and linear for α. Most of the existing rain attenuation prediction models use regression coefficients k and α to estimate the rain attenuation.

The further theoretical backgrounds are highlighted in [29] along with a brief overview of the Simple Attenuation Model (SAM). SAM model studies the relationship among specific attenuation and rain rate, statistics of the point rainfall intensity and spatial distribution of rainfall on earth-space communication links operating in the range of 10 to 35 GHz. The effective path length is calculated from an effective rain height which is expressed by Equations (3a) and (3b). In stratiform rain, with point $R \leq 10$ mm/hr, the rain height is constant and equal to isotherm height above mean sea level whose values is given by ITU-R P. 839-4 [21]. Similarly, in convective rainstorms, when $R > 10$ mm/hr, the effective rain height depends on the rain rate because strong storms push rain higher into the atmosphere, lengthening the slant path. The attenuation time series is depicted as [22],

$$A_{p\%} = \gamma L_s; \quad R_{p\%} \leq 10\,\text{mm/hr} \tag{3}$$

$$L_s = (H_R - H_S)/\sin\theta \tag{3a}$$

where $A_{p\%}$ and $R_{p\%}$ are the attenuation and rain rate exceeded for $p\%$ of time; γ is the specific attenuation due to rainfall; L_s is the slant-path length up to rain height; H_R is the rain height above mean sea level; H_s is the station height; θ is the elevation angle of the top of rain height.

In convective rainstorms, when $R_{p\%} > 10$ mm/hr, a modified value of effective path length is used for determination of slant path attenuation as:

$$A_{p\%} = \gamma \frac{1 - \exp\left[-ab\ln(R_{p\%}/10)\right] L_s \cos\theta}{ab\ln(R_{p\%}/10)\cos\theta}; \quad R_{p\%} > 10\,\text{mm/hr} \tag{3b}$$

where $b = 1/22$. Furthermore, the empirical expression for effective rain height H_R is given as:

$$H_R = \begin{cases} H_0; & R \leq 10\,\text{mm/hr} \\ H_0 + \log\left(\dfrac{R}{10}\right); & R > 10\,\text{mm/hr} \end{cases} \tag{3c}$$

H_0 is the 0°C isotherm height. The detailed description on the applicability of this model is described in [22].

Furthermore, Table 1 shows the local rain rate statistics, as given in ITU-R P. 837-7 [35] which is considered as part of the input parameters for the prediction methods. The table shows that the rain rate is higher particularly in the months of April, May, June, July, August, September, October and November. Hence, these months' statistics are studied in the further section.

3. EXPERIMENTAL METHODS

The propagation measurements over an earth space path have been carried out at Korea Radio Promotion Association building, Mokdong-13 na-gil, Yangcheong-gu, Seoul, Republic of Korea (37°32'45.25"N, 126°52'58.8"E) by National Radio Research Agency, RRA by receiving a Ku and Ka bands beacon signals of the Koreasat 6 satellite at 12.25 and 20.73 GHz, respectively, using 1.8 m antenna whose specification is detailed [29]. Similarly, another beacon receiver is installed at same place to measure the Ka band beacon at 19.8 GHz from COMS 1 using a similar sized antenna whose specifications are depicted in Table 2.

The receiver samples the data that are measured for 10 seconds interval, which are averaged over 1-minute distribution for further statistical analysis with the averaging method as mentioned in [17]. The Ka-band signal is down converted to an intermediate frequency signal using a low noise block (LNB)

Table 1. Local rain rate statistics for obtained from the combined rain rate values from 2013 to 2016 [23].

Time	Rain Rate (mm/hr)					
Percentage	January	February	March	April	May	June
1	0.16	0.10	0.03	0.32	0.84	0.10
0.5	0.26	0.23	0.05	0.45	0.98	0.26
0.3	0.35	0.53	0.09	0.54	1.16	1.54
0.2	0.56	0.64	0.10	0.67	1.26	1.85
0.1	0.68	0.88	0.12	0.88	1.36	1.91
0.05	0.77	0.95	0.24	1.45	2.60	2.09
0.03	1.17	1.88	0.68	1.96	3.62	2.92
0.02	1.45	2.67	1.08	2.38	4.26	3.76
0.01	2.09	3.86	1.69	3.12	5.61	6.30
0.005	2.94	4.93	2.09	4.01	7.02	11.93
0.003	3.77	6.04	2.43	5.34	8.17	19.08
0.002	4.81	7.22	2.71	6.66	9.43	26.06
0.001	6.79	8.28	3.17	13.46	12.27	33.07
Time	**Rain Rate (mm/hr)**					
Percentage	**July**	**August**	**September**	**October**	**November**	**December**
1	0.26	0.58	0.98	0.68	0.78	0.32
0.5	0.98	0.98	1.12	0.77	0.83	0.45
0.3	1.07	1.15	1.32	0.87	0.98	0.54
0.2	2.30	1.24	1.45	0.98	1.02	0.65
0.1	6.07	1.43	1.61	1.07	1.12	0.74
0.05	13.67	3.67	3.18	1.17	1.76	0.95
0.03	20.94	5.89	4.72	2.06	2.30	1.02
0.02	27.05	8.19	6.30	2.72	2.77	1.23
0.01	37.67	17.34	10.46	4.07	3.68	1.63
0.005	46.39	38.76	17.73	6.69	4.65	2.26
0.003	53.54	58.03	26.43	10.33	5.55	2.70
0.002	59.47	71.23	33.83	12.50	6.91	3.16
0.001	71.61	85.58	43.03	19.32	10.80	4.06

converter having a noise figure of 1.5 dB. The output at LNB was fed to a signal selector, which selected the appropriate signal that range from 10 kHz to 26.5 GHz. After selecting the appropriate beacon signal, the output was fed to a spectrum analyzer via RG-11 coaxial cable at a sampling rate of one sample every 10 second. Finally, the output of spectrum analyzer was sent to the computer via general purpose interface bus cable and then stored using a data logger. The unattenuated beacon signal level was used to provide a reference level in dBm, which was the average signal power received under clear sky conditions. During rain, the attenuation was estimated by measuring the excess attenuation over the clear weather attenuation values at respective rain rates. For instance, attenuation is calculated by subtracting the clear sky signal power from the measured excess attenuation value at that instant. The rainfall rate was measured using an OTT Parsivel, a laser optical disdrometer for simultaneous measurement of particle size and velocity of all liquid and solid precipitation. The transmitter unit of the sensor generates a flat, horizontal beam of light, which the receiver unit converts into an electrical signal. This signal changes whenever a hydrometeor falls through the beam anywhere within the measurement area. The Particle Size and Velocity (PARSIVEL) disdrometer is a laser based instrument designed to count and measure simultaneously the size and fall speed of precipitation particles. The descriptions of the experimental

Table 2. Specifications of the 19.8 GHz link for COMS1 satellite link.

Type	Descriptions	Specification
System Location	Location	37.5459°N, 126.883°E
	Elevation angle	46.5°
	Azimuth angle	177.8°
	Sea level (km)	0.055
Receiver Antenna	Antenna type	Off-set parabolic
	Frequency Band (GHz)	$10.95 \sim 31$
	Beacon signal level for clear sky	-73.4 dBm
	Polarization	Vertical
	Gain	$55\,\text{dB} \pm 2\,\text{dB}$

equipment, topographic parameters of the link, experimental geometry and data acquisition technique have been reported in [18, 29, 30]. The limitations of Parsivel disdrometer are the limited sampling, the possibility to have multiple drops passing through the sampling area at same instance of time and the axis ratio considered for drop equivolumetric diameter retrieval. In order to reduce the probability of multiple drop, there have been the limited sampling area of Parsivel. Additionally, the splashing of drops on the head of the sensor can induce non-natural small drops. Due to the shape of instrument, strong wind might have an effect on Parivel measurements, in particular for small drops [23].

The detailed diagram for setup of the system is shown in Figure 1.

Similarly, Figure 2 shows the sample record of the simultaneous measurement of received signal level and rain rate for 19.8 GHz.

This paper considers the analyses performed in monthly and diurnal variation of 19.8 GHz satellite links. Similarly, the measurements performed for 2013 year for mentioned three satellite links are used for studying frequency scaling approach. The methods applied to derive the cumulative distribution of slant path attenuation and 1-minute rain rate for each year and when combined together are mentioned in [18]. The monthly variation of 1-minute integrated data for given time percentage are obtained by taking the samples that correspond to the instance of values calculated, which results from the product of number of years, days in a month, hours in a day, minutes with corresponding time percentage. For instance, in 0.1% of time percentage, the required value is obtained as $(1 \times 30 \times 24 \times 60 \times 0.1 \div 100) = 43.2 \approx 43$. Figures 3(a), (b), (c), (d) and Figures 4(a), (b), (c), (d) represent the monthly variations of rain attenuation and rain rate for four consecutive years 2013, 2014, 2015, 2016 respectively for 19.8 GHz link.

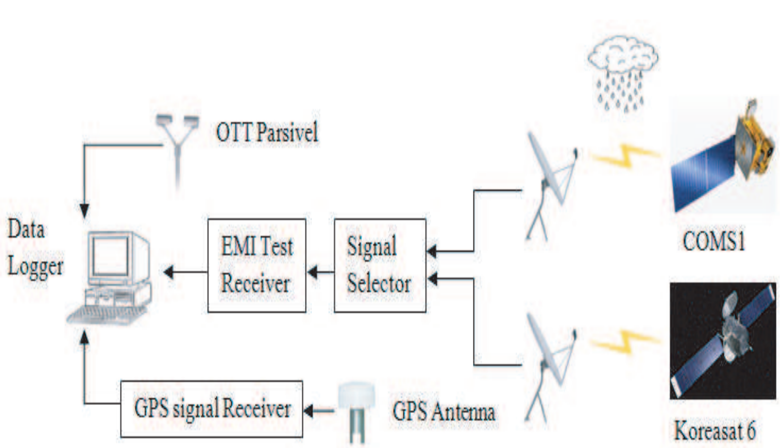

Figure 1. Experimental setup of rain attenuation and rain rate measurement [23].

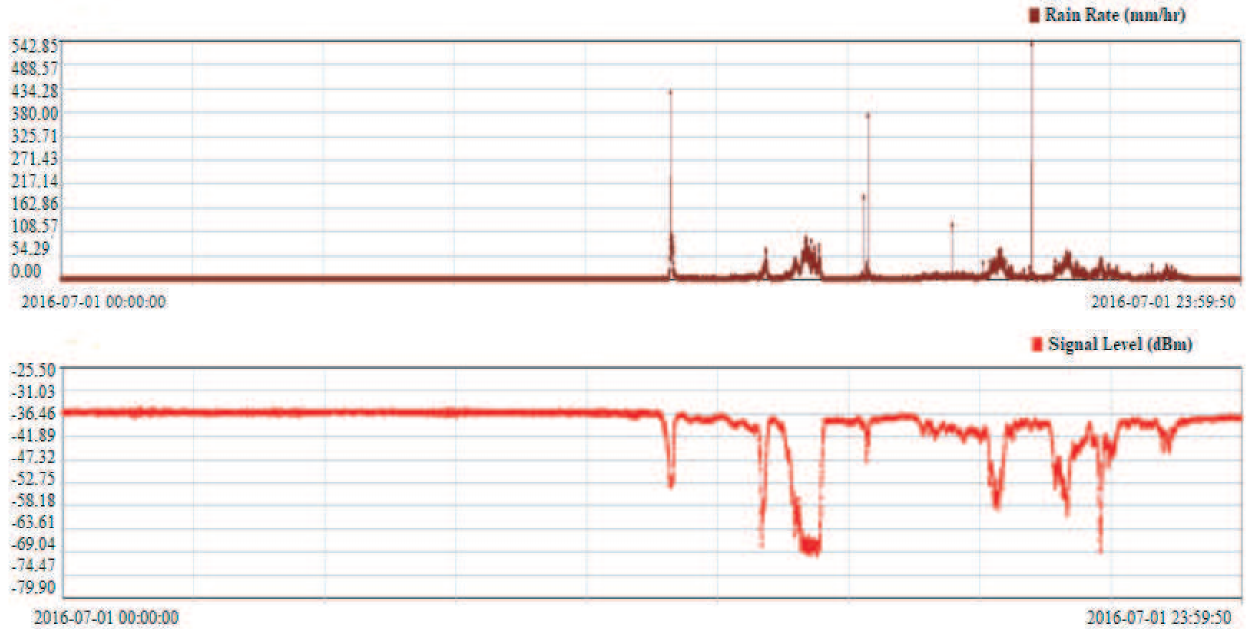

Figure 2. Variation of 19.8 GHz signal attenuation during a rain event [23].

The relative trends of better curves are shown in 2013 where as for successive three years, higher rain attenuation and rain rate values are observed particularly in the months of June, July, August, September and October as noticed from Figures 3(a), (b), (c), (d), Figures 4(a), (b), (c), (d) and Figures 5(a), (b). This might be because of the measurement of data performed for 5-second instances which have been combined for 1-minute distribution. Interestingly, the distribution of rain rate against rain attenuation as observed from Figure 5(c) indicates that there is a positive correlation between the rain rate and rain attenuation. In order to derive Figure 5(c), we have arranged cumulative distributions of rain rate and rain attenuation for four consecutive years from 2013 to 2016 with the time percentage ranging from 1% to 0.001%. Hence the obtained rain rate and rain attenuation statistics are plotted along the x-axis and y-axis, respectively, which show the curve nature presented in Figure 5(c). The mentioned months of June, July, August and September have been considered because in this time period the rainfall is observed greater over this region. The average monthly rainfall accumulation for the three years of measurement is shown in Figure 6 which reveals that maximum average monthly rainfall accumulation is observed in the months of July and August. In addition, month-wise variability of rain rate and rain attenuation is studied further to generalize the use of regression coefficients k and α values for better estimation against the measured rain attenuation statistics.

4. RESULTS AND DISCUSSION

The analysis presented above is applied to numerically illustrate the relation between estimated and measured rain attenuations. To this end, the Complementary Cumulative Distribution Function (CCDF) for rain attenuation of four years at 19.8 GHz, calculated with the ITU-R P. 618-13 prediction using k and α values as recommended by ITU-R P. 838-3 and proposed attenuation obtained from the product of effective path length and specific attenuation values as calculated with the use of empirically generated regression coefficients k and α are shown in Figures 7(a), (b), (c) and (d) in several time percentages, P, at equiprobable exceedance probability ($0.001\% \leq P \leq 1\%$) for winter, spring, summer and fall seasons, respectively.

As shown in Figures 7(a), 7(b) for winter and spring seasons, ITU-R P. 618-13 and SAM models show underestimation against the measured values whereas the proposed method gives a closer estimation. Similarly for the months of June and November, ITU-R P. 618-13 and SAM give the underestimation where these models overestimate in July, August, September and October months as noticed from Figures 7(c) and 7(d). Figure 8(a) presents the diurnal rain attenuation pattern which depicts the less attenuation values during late night time from 18 to 24 hours, whereas for other time instances there are higher attenuation values for 2013. Similarly, the diurnal rain rate distribution is

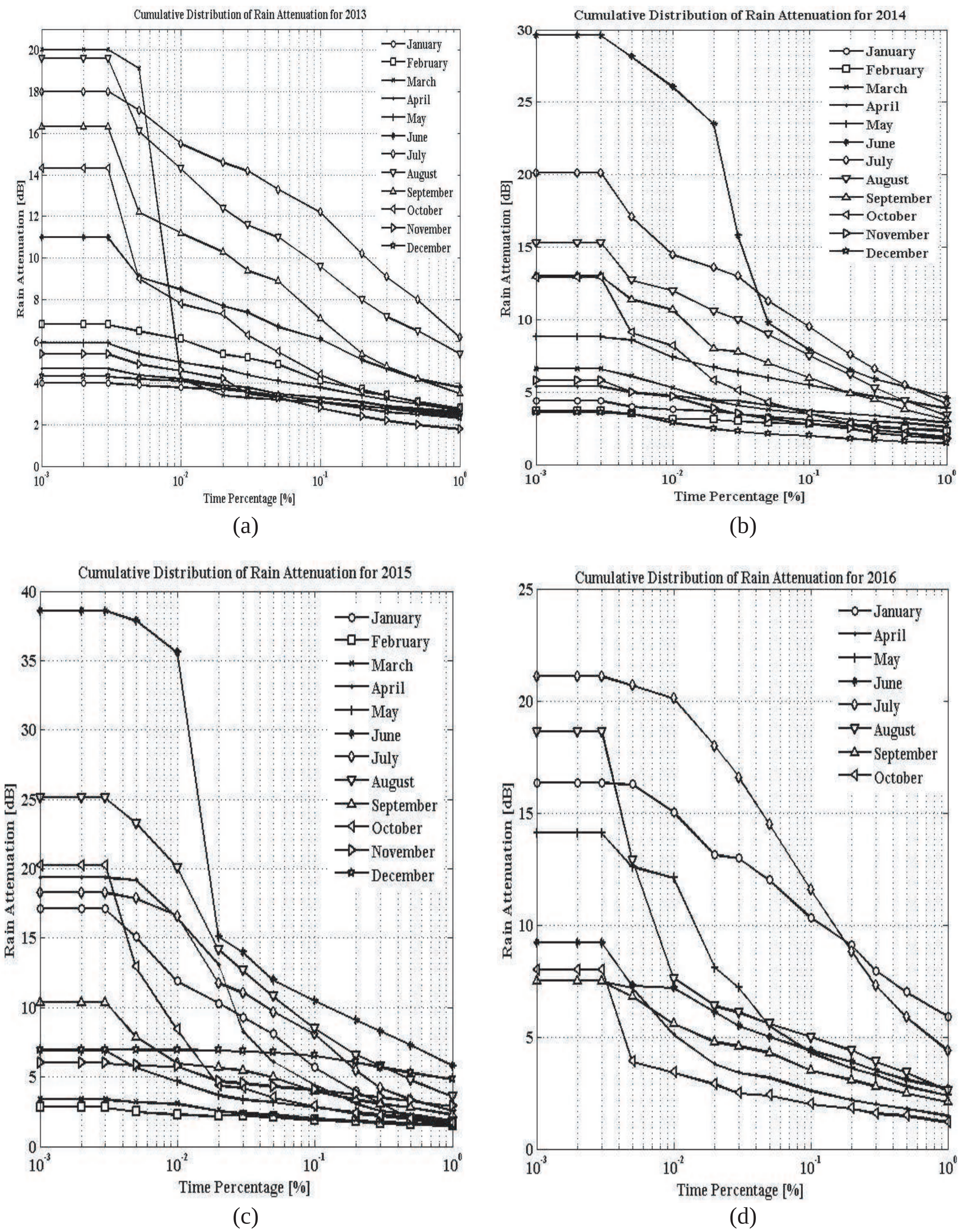

Figure 3. (a) Distribution of rain attenuation for 2013. (b) Distribution of rain attenuation for 2014. (c) Distribution of rain attenuation for 2015. (d) Distribution of rain attenuation for 2016.

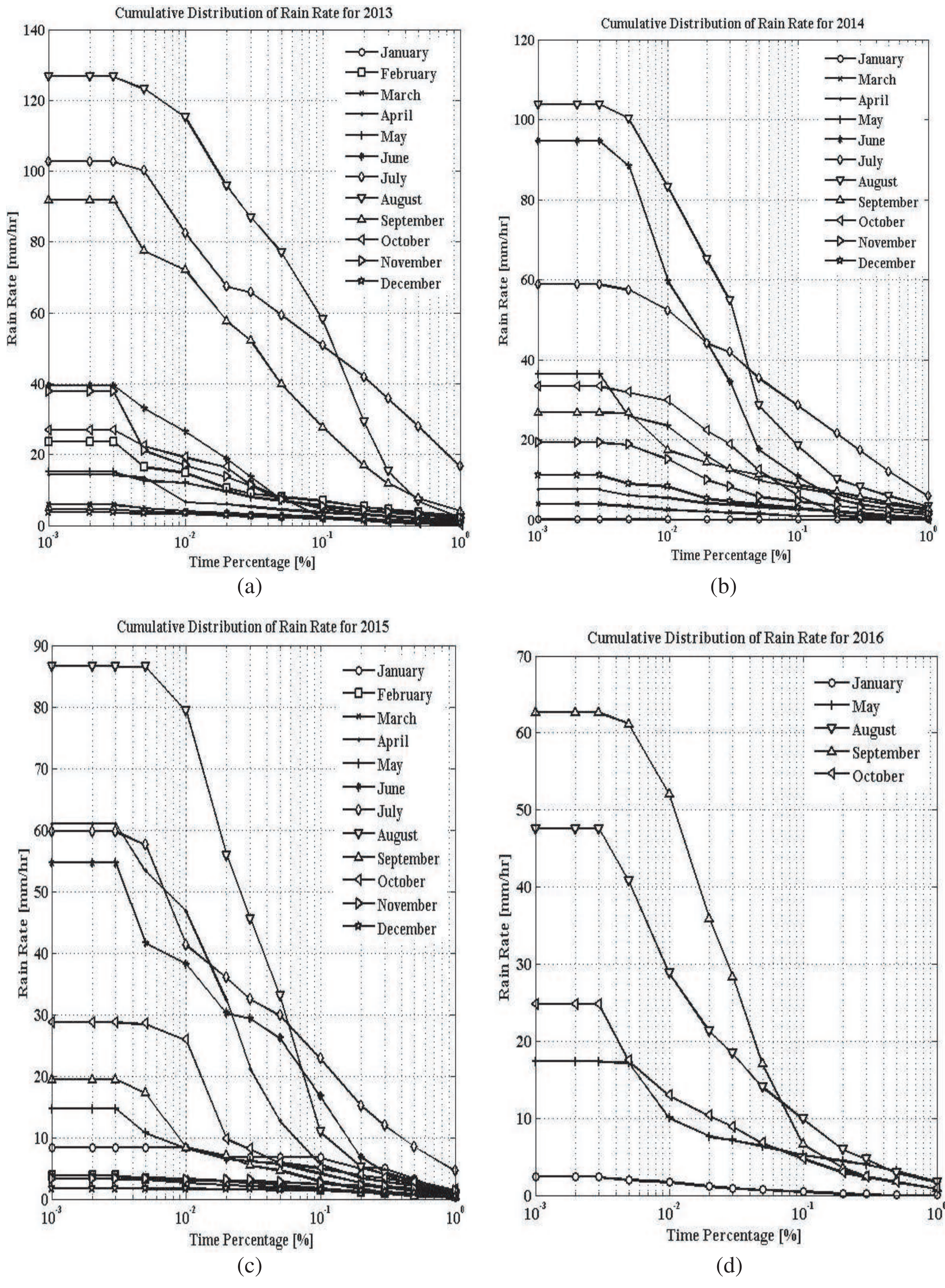

Figure 4. (a) Rainfall rate distribution for 2013. (b) Rainfall rate distribution for 2014. (c) Rainfall rate distribution for 2015. (d) Rainfall rate distribution for 2016.

shown in Figure 8(b) which highlights similar facts where there is lower values of rain rate for late night time from 18 to 24 hours, whereas for other time instances, there is higher values of ran rate. We have maintained the duration of 24 hours with four intervals such as 0–6, 6–12, 12–18 and 18–24. Due to the

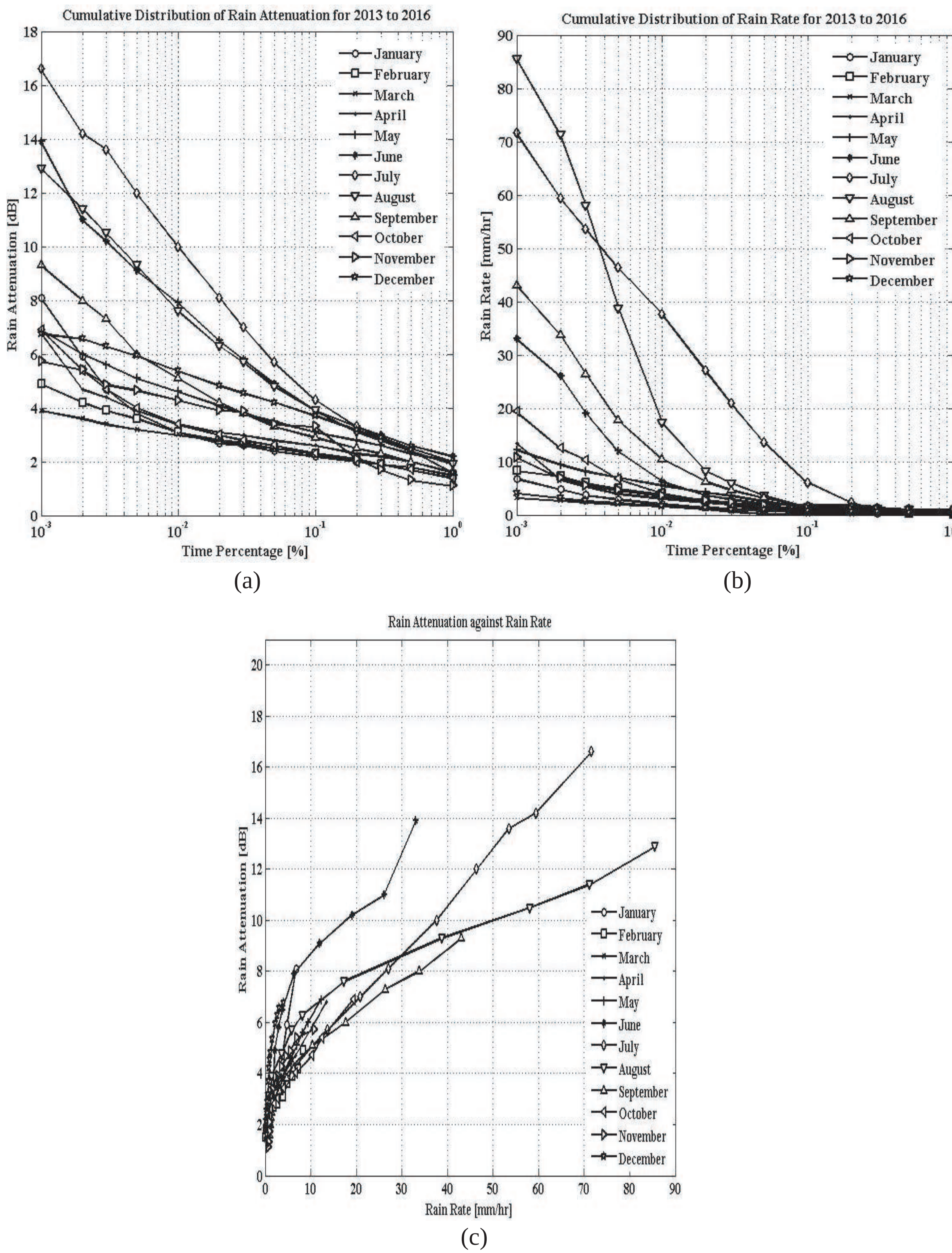

Figure 5. (a) Rain attenuation distribution. (b) Rain rate distribution. (c) Rain attenuation against rain rate distribution.

better statistical data arrangement in 2013 year, this period has been chosen for the study of diurnal variation. Better analyses can be determined by the values of error matrices in further part.

The empirically generated regression coefficients, k and α, for 19.8 GHz links as calculated from the statistical calculation of the data obtained for the four years, 2013 till 2016 are tabulated in Table 3. Similarly, the obtained values for effective path length, derived from the rain rate values as described in the SAM approach, are depicted in Table 4. The values are constant for most of the time percentage because of the rain rate whose values are lower than 10 mm/hr. The correlation coefficient, R^2, is greater for the proposed method which indicates a better estimation of rain attenuation from rain rate statistics. The effective length is obtained from SAM approach whose inverse is multiplied with measured rain attenuation statistics. Hence, it is plotted against the measured rain rate statistics from where the required values of k and α are calculated. The rain attenuation is thus calculated with the product of empirically generated k and α values, with estimated, L_{eff}. Similarly, k and α are also derived from the procedure explained in ITU-R P. 838-3 which are used to obtained attenuation values for ITU-R P. 618-13 extrapolation approach. Hence, comparison of the attenuation obtained from empirically generated k and α along with the ITU-R P. 618-13 prediction method is studied for the combined rain rate and rain attenuation statistics for 2013, 2014, 2015 and 2016 years. The further error analyses support the judgment of mentioned approaches.

The rain attenuation prediction model for Earth-satellite link is determined for exceeding time percentages in the range 0.001% to 1%. Hence, the percentage errors, $\varepsilon(P)$, between measured Earth-satellite attenuation data ($A_{\%p,\,\text{measured}}$) in dB and the model's predictions ($A_{\%p,\,\text{predicted}}$) in dB are obtained with expression exceeding time percentage of interest on link at the same probability level, P, in the percentage interval $10^{-3}\% < P < 1\%$, as follows:

$$\varepsilon(P)_T = \frac{A_{\%p,\,\text{predicted}} - A_{\%p,\text{measured}}}{A_{\%p,\,\text{measured}}} \times 100\ [\%] \tag{4}$$

In addition, Chi-Square statistic is used to access the methods performance which is given by Equation (5).

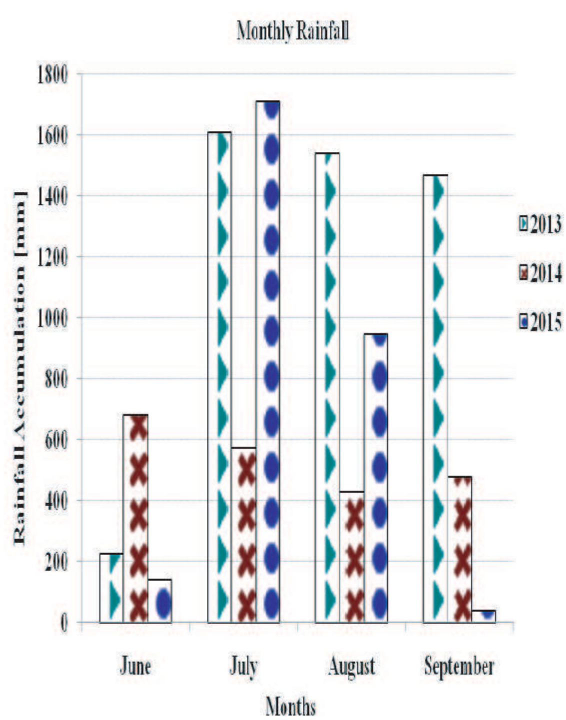

Figure 6. Monthly average of rainfall amount for three years of measurement [23].

Chi-Square statistic is defined as [26]:

$$\chi^2 = \sum_{i=1}^{N} \frac{\left(A_{\%p,\,\mathrm{predicted},\,i} - A_{\%p,\,\mathrm{measured},\,i}\right)^2}{A_{\%p,\,\mathrm{predicted},\,i}} \tag{5}$$

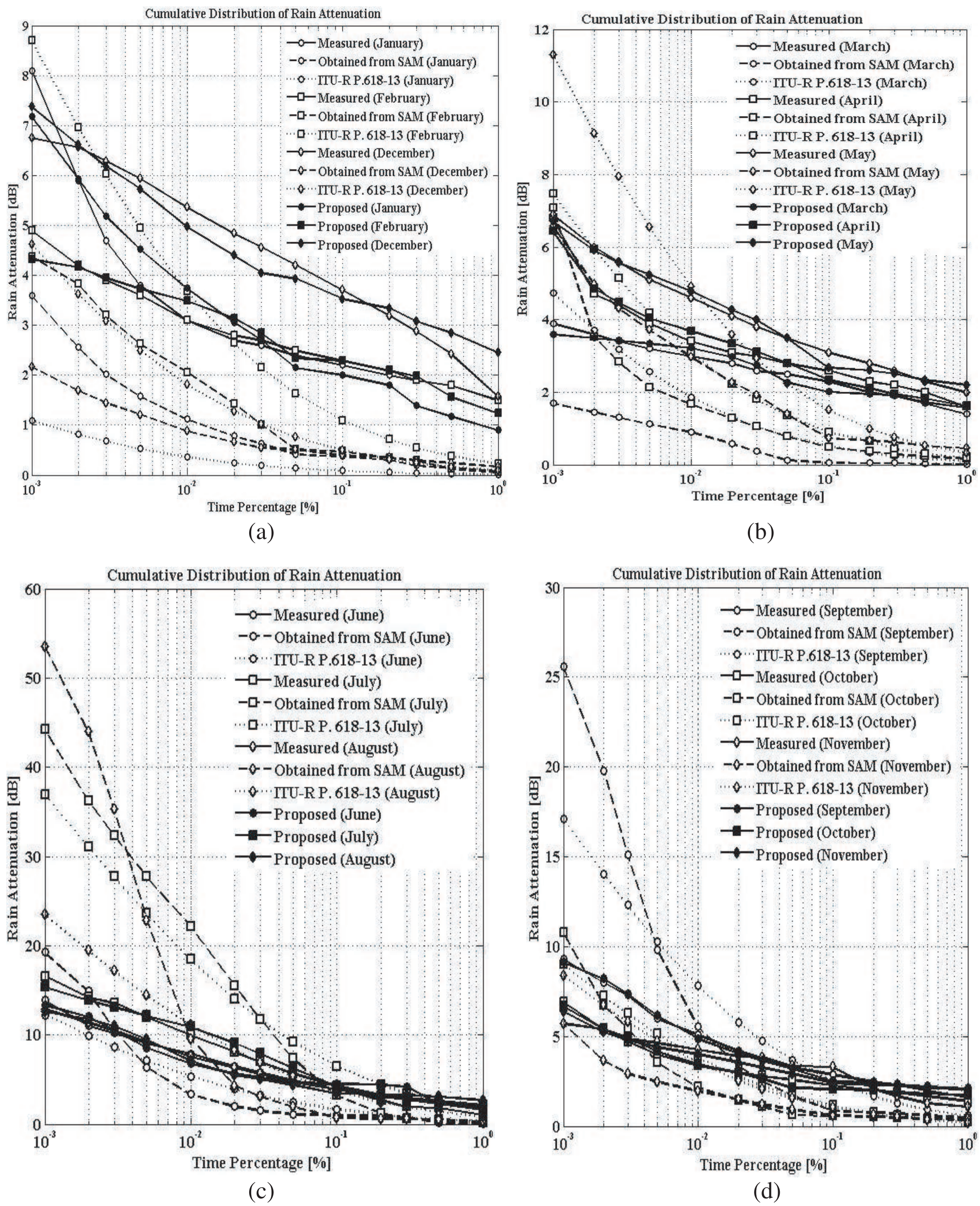

Figure 7. (a) Distribution of rain attenuation as compared with other models for winter. (b) Distribution of rain attenuation as compared with other models for spring. (c) Distribution of rain attenuation as compared with other models for summer. (d) Distribution of rain attenuation as compared with other models for fall.

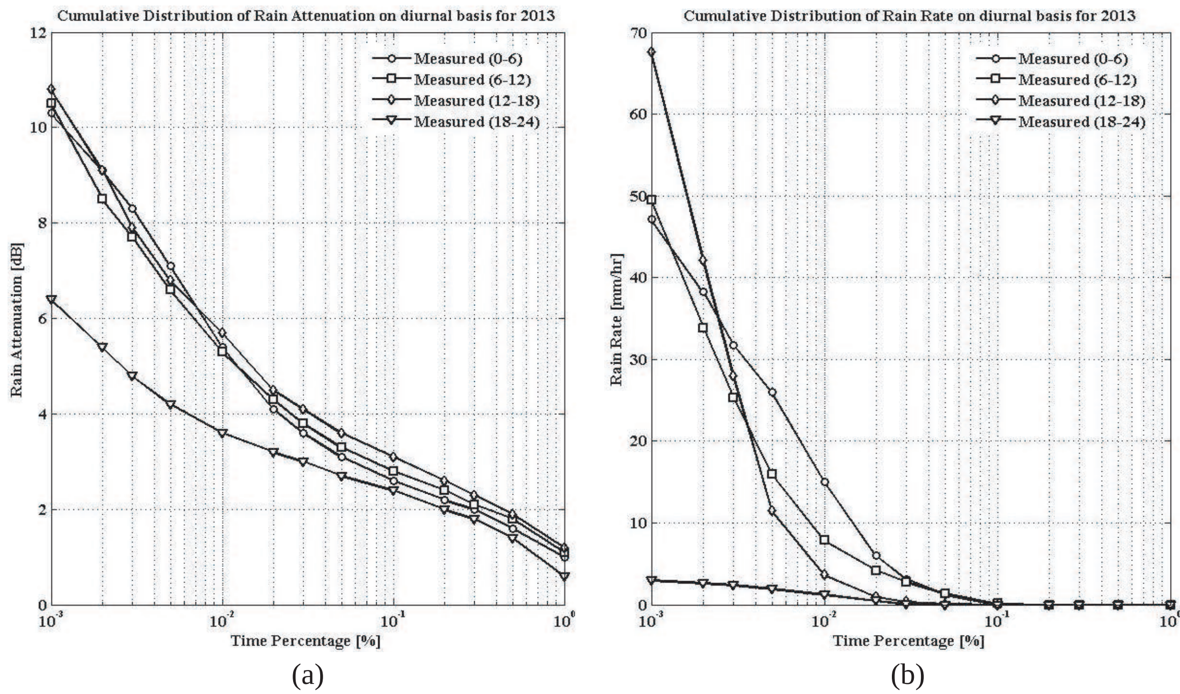

Figure 8. (a) Distribution of rain attenuation based on diurnal variation [23]. (b) Distribution of rain rate based on diurnal variation [23].

Table 3. Regression coefficients for three satellite links [24].

Month	R^2	k	α
January	0.9255	0.4307	0.5528
February	0.9372	0.411	0.2835
March	0.9456	0.5076	0.1766
April	0.9767	0.4233	0.3606
May	0.9842	0.4094	0.4076
June	0.9426	0.6328	0.3367
July	0.967	0.3268	0.4471
August	0.9661	0.5442	0.2671
September	0.9876	0.3704	0.3482
October	0.9804	0.3508	0.38
November	0.8567	0.3995	0.4243
December	0.9353	0.6963	0.4324

Similarly, for standard deviation, STD, and root mean square, RMS calculation, the approaches followed in [14] have been adopted. The calculated relative error probability, $\varepsilon(P)$, standard deviation, STD, root mean square, RMS, and Chi-Square values are tabulated. As per the recommendation by ITU-R P. 311-15 [25], the ratio of predicted to measured attenuation is calculated, and the natural logarithm of these error ratios is used as a test variable. The mean (μ_v), standard deviation (σ_v) and root mean square (ρ_v) of the test variable are then calculated to provide the statistics for prediction method's comparison, which are listed in Tables 5–8 along with the evaluation procedures adopted for comparison of prediction methods by the recommendation ITU-R P. 311-15 [25]. The proposed empirically derived k and α, used in specific attenuation calculation which is used to obtained desired attenuation values, results have

Table 4. Estimated effective path length.

Time Percentage	L_{eff}					
	January	February	March	April	May	June
1	5.78322059	5.78322059	5.78322059	5.78322059	5.78322059	5.78322059
0.5	5.78322059	5.78322059	5.78322059	5.78322059	5.78322059	5.78322059
0.3	5.78322059	5.78322059	5.78322059	5.78322059	5.78322059	5.78322059
0.2	5.78322059	5.78322059	5.78322059	5.78322059	5.78322059	5.78322059
0.1	5.78322059	5.78322059	5.78322059	5.78322059	5.78322059	5.78322059
0.05	5.78322059	5.78322059	5.78322059	5.78322059	5.78322059	5.78322059
0.03	5.78322059	5.78322059	5.78322059	5.78322059	5.78322059	5.78322059
0.02	5.78322059	5.78322059	5.78322059	5.78322059	5.78322059	5.78322059
0.01	5.78322059	5.78322059	5.78322059	5.78322059	5.78322059	5.78322059
0.005	5.78322059	5.78322059	5.78322059	5.78322059	5.78322059	5.79546626
0.003	5.78322059	5.78322059	5.78322059	5.78322059	5.78322059	5.80562323
0.002	5.78322059	5.78322059	5.78322059	5.78322059	5.78322059	5.79521545
0.001	5.78322059	5.78322059	5.78322059	5.80111614	5.79694524	5.77854207
Time Percentage	L_{eff}					
	July	August	September	October	November	December
1	5.78322059	5.78322059	5.78322059	5.78322059	5.78322059	5.78322059
0.5	5.78322059	5.78322059	5.78322059	5.78322059	5.78322059	5.78322059
0.3	5.78322059	5.78322059	5.78322059	5.78322059	5.78322059	5.78322059
0.2	5.78322059	5.78322059	5.78322059	5.78322059	5.78322059	5.78322059
0.1	5.78322059	5.78322059	5.78322059	5.78322059	5.78322059	5.78322059
0.05	5.80170329	5.78322059	5.78322059	5.78322059	5.78322059	5.78322059
0.03	5.80391614	5.78322059	5.78322059	5.78322059	5.78322059	5.78322059
0.02	5.79310049	5.78322059	5.78322059	5.78322059	5.78322059	5.78322059
0.01	5.76637203	5.80612636	5.7867471	5.78322059	5.78322059	5.78322059
0.005	5.74259012	5.76342499	5.8061247	5.78322059	5.78322059	5.78322059
0.003	5.72326454	5.71135979	5.79443814	5.7851152	5.78322059	5.78322059
0.002	5.70759404	5.67791079	5.77656224	5.7978905	5.78322059	5.78322059
0.001	5.67699068	5.64421687	5.75177373	5.80546841	5.8909926	5.78322059

lower chances of error than ITU-R P. 618-13 approach when $0.001\% \leq P \leq 1\%$ which is justified from lower STD, RMS, χ^2 values. Thus, for all time percentages when $0.001\% \leq P \leq 1\%$, for 19.8 GHz, empirically derived k and α values can be used. As noted from Tables 5–8 for winter, spring, summer and fall seasons in 19.8 GHz link, ITU-R P. 618-13 shows the relative error percentages of 96%, 88%, 86%; 52%, 19%, 78%; 86%, 66%, 32% for January, February, December months; 77%, 38%, 21%; 65%, 9%, 10%; 51%, 7%, 64% for March, April, May months; 57%, 32%, 12%; 51%, 85%, 123%; 4%, 47%, 82% for June, July, August months; 13%, 53%, 84%; 50%, 13%, 31%; 68%, 17%, 47% for September, October, November months at 0.1%, 0.01% and 0.001% of the time respectively. Similarly, SAM approach results in 83%, 64%, 56%; 79%, 34%, 11%; 89%, 84%, 68% for January, February, December months; 97%, 70%, 56%; 81%, 51%, 4%; 76%, 35%, 5% for March, April, May months; 74%, 58%, 39%; 25%, 122%, 167%; 80%, 26%, 315% for June, July, August months; 70%, 9%, 175%; 75%, 36%, 56%; 82%, 54%, 0% for September, October, November months at 0.1%, 0.01% and 0.001% of the time respectively. In the other hand, the proposed method gives 9%, 21%, 11%; 0%, 12%, 12%; 5%, 7%, 9% for January, February, December months; 12%, 7%, 8%; 10%, 9%, 5%; 14%, 4%, 3% for March, April, May months; 17%, 14%, 4%; 2%, 9%, 7%; 11%, 6%, 2% for June, July, August months; 13%, 4%, 2%; 9%, 2%, 3%; 27%, 6%, 12% for September, October, November months at 0.1%, 0.01% and 0.001% of the time, respectively. Furthermore, use of the proposed empirical coefficients k and α results in lower values of μ_v for 19.8 GHz link, as per the recommendation of ITU-R P. 311-15 [25] which is justified from lower values of σ_v and ρ_v. Thus, these emphasize the suitability of proposed empirical coefficients for the estimation of rain attenuation in slant path for earth space communication in 19.8 GHz link.

Table 5. Percentage error obtained over the interval [0.001% to 1%] for winter season.

Months	Methods	Parameters	Time Percentage (% p)													ITU-R P.311-15		
			1	0.5	0.3	0.2	0.1	0.05	0.03	0.02	0.01	0.005	0.003	0.002	0.001	μ_v	σ_v	ρ_v
January	ITU-R P. 618-13	ε(P)	-0.99	-0.99	-0.98	-0.97	-0.96	-0.94	-0.93	-0.91	-0.88	-0.86	-0.86	-0.86	-0.86	-2.21	0.52	2.27
		STD	0.07	0.06	0.06	0.05	0.04	0.02	0.00	0.01	0.04	0.06	0.07	0.06	0.06			
		RMS	1.49	1.77	1.86	1.95	2.11	2.26	2.41	2.45	2.73	3.27	4.02	5.08	7.00			
		χ^2	151.81	123.26	90.87	73.12	52.08	37.17	30.35	24.59	20.45	20.26	23.81	31.55	44.61			
	SAM	ε(P)	-0.94	-0.92	-0.90	-0.85	-0.83	-0.83	-0.76	-0.71	-0.64	-0.58	-0.57	-0.57	-0.56	-1.17	0.41	1.24
		STD	0.20	0.18	0.16	0.10	0.09	0.08	0.01	0.03	0.10	0.16	0.17	0.18	0.19			
		RMS	1.41	1.66	1.71	1.69	1.83	1.98	1.97	1.91	1.98	2.22	2.68	3.34	4.50			
		χ^2	22.28	19.01	15.07	9.32	8.98	9.37	6.09	4.66	3.47	3.13	3.58	4.35	5.61			
	Proposed Method	ε(P)	-0.40	-0.34	-0.27	-0.10	-0.09	-0.10	0.04	0.13	0.21	0.19	0.10	0.01	-0.11	0.02	0.15	0.16
		STD	0.34	0.29	0.21	0.04	0.03	0.05	0.10	0.19	0.26	0.25	0.16	0.06	0.06			
		RMS	0.60	0.62	0.51	0.19	0.19	0.25	0.11	0.36	0.64	0.72	0.49	0.03	0.92			
		χ^2	0.39	0.32	0.18	0.02	0.02	0.03	0.00	0.04	0.11	0.12	0.05	0.00	0.12			
February	ITU-R P. 618-13	ε(P)	-0.84	-0.79	-0.71	-0.66	-0.52	-0.35	-0.20	-0.05	0.19	0.37	0.54	0.66	0.78	-0.27	0.58	0.64
		STD	0.72	0.66	0.59	0.54	0.40	0.22	0.08	0.07	0.31	0.50	0.67	0.78	0.90			
		RMS	1.26	1.41	1.35	1.39	1.20	0.86	0.55	0.15	0.58	1.34	2.12	2.76	3.80			
		χ^2	6.78	5.19	3.36	2.70	1.32	0.46	0.14	0.01	0.09	0.36	0.75	1.10	1.66			
	SAM	ε(P)	-0.96	-0.93	-0.85	-0.83	-0.79	-0.79	-0.62	-0.49	-0.34	-0.27	-0.18	-0.09	-0.11	-0.87	0.68	1.11
		STD	0.41	0.37	0.29	0.28	0.23	0.23	0.07	0.07	0.22	0.29	0.38	0.47	0.45			
		RMS	1.44	1.67	1.61	1.75	1.82	1.98	1.69	1.36	1.04	0.98	0.69	0.38	0.52			
		χ^2	37.10	21.89	8.89	8.73	6.90	7.55	2.80	1.30	0.52	0.36	0.15	0.04	0.06			
	Proposed Method	ε(P)	-0.18	-0.13	0.04	0.00	0.00	-0.06	0.05	0.12	0.12	0.04	0.01	-0.01	-0.12	0.00	0.07	0.07
		STD	0.17	0.12	0.05	0.01	0.00	0.05	0.06	0.13	0.13	0.05	0.02	0.00	0.11			
		RMS	0.26	0.23	0.09	0.01	0.01	0.16	0.14	0.34	0.38	0.14	0.06	0.04	0.57			
		χ^2	0.06	0.03	0.00	0.00	0.00	0.01	0.01	0.04	0.04	0.00	0.00	0.00	0.08			
December	ITU-R P. 618-13	ε(P)	-0.94	-0.93	-0.92	-0.90	-0.86	-0.82	-0.77	-0.74	-0.66	-0.58	-0.51	-0.45	-0.32	-1.26	0.55	1.38
		STD	0.21	0.21	0.19	0.18	0.14	0.10	0.05	0.01	0.06	0.14	0.21	0.27	0.41			
		RMS	1.48	2.26	2.64	2.87	3.21	3.44	3.53	3.56	3.55	3.44	3.20	2.95	2.13			
		χ^2	21.72	30.36	28.69	25.71	20.40	15.40	12.12	9.88	6.94	4.74	3.30	2.40	0.98			
	SAM	ε(P)	-0.89	-0.90	-0.90	-0.89	-0.89	-0.88	-0.88	-0.86	-0.84	-0.80	-0.77	-0.74	-0.68	-1.58	0.24	1.59
		STD	0.05	0.06	0.06	0.05	0.05	0.04	0.04	0.02	0.00	0.04	0.07	0.10	0.16			
		RMS	1.40	2.18	2.58	2.83	3.31	3.69	4.01	4.17	4.49	4.72	4.84	4.88	4.59			
		χ^2	11.12	19.23	22.51	22.56	27.01	26.34	29.07	26.12	22.78	18.32	16.15	14.06	9.72			
	Proposed Method	ε(P)	0.56	0.17	0.07	0.05	-0.05	-0.06	-0.11	-0.09	-0.07	-0.04	-0.02	0.01	0.09	0.02	0.10	0.11
		STD	0.52	0.13	0.03	0.01	0.09	0.10	0.15	0.13	0.11	0.07	0.06	0.03	0.05			
		RMS	0.88	0.42	0.20	0.15	0.17	0.27	0.51	0.44	0.39	0.21	0.10	0.05	0.62			
		χ^2	0.31	0.06	0.01	0.01	0.01	0.02	0.06	0.04	0.03	0.01	0.00	0.00	0.05			

Table 6. Percentage error obtained over the interval [0.001% to 1%] for spring season.

Months	Methods	Parameters	Time Percentage (% p)													ITU-R P.311-15		
			1	0.5	0.3	0.2	0.1	0.05	0.03	0.02	0.01	0.005	0.003	0.002	0.001	μ_v	σ_v	ρ_v
March	ITU-R P. 618-13	ε(P)	-0.93	-0.90	-0.87	-0.84	-0.77	-0.68	-0.59	-0.53	-0.38	-0.20	-0.07	0.03	0.21	-0.75	0.63	0.98
		STD	0.43	0.40	0.37	0.33	0.27	0.18	0.09	0.03	0.12	0.30	0.43	0.53	0.71			
		RMS	1.30	1.53	1.65	1.67	1.78	1.71	1.54	1.48	1.13	0.64	0.23	0.11	0.84			
		χ^2	16.16	13.42	10.90	8.46	6.12	3.70	2.25	1.67	0.69	0.16	0.02	0.00	0.15			
	SAM	ε(P)	-0.99	-0.98	-0.97	-0.97	-0.97	-0.95	-0.86	-0.79	-0.70	-0.65	-0.62	-0.60	-0.56	-1.74	0.88	1.95
		STD	0.17	0.17	0.16	0.16	0.16	0.13	0.04	0.03	0.12	0.17	0.20	0.22	0.25			
		RMS	1.38	1.67	1.85	1.94	2.23	2.37	2.23	2.21	2.09	2.07	2.10	2.14	2.20			
		χ^2	111.59	98.52	67.53	67.24	74.12	42.36	13.38	8.34	4.79	3.82	3.37	3.15	2.86			
	Proposed Method	ε(P)	0.13	0.02	0.01	-0.02	-0.12	-0.09	0.05	0.06	0.07	0.04	0.01	-0.03	-0.08	0.00	0.05	0.05
		STD	0.12	0.01	0.01	0.03	0.13	0.09	0.05	0.06	0.07	0.04	0.00	0.03	0.08			
		RMS	0.18	0.03	0.02	0.05	0.28	0.22	0.14	0.18	0.22	0.14	0.03	0.10	0.30			
		χ^2	0.02	0.00	0.00	0.00	0.04	0.02	0.01	0.01	0.01	0.01	0.00	0.00	0.03			
April	ITU-R P. 618-13	ε(P)	0.88	-0.84	-0.80	-0.71	-0.65	-0.51	-0.40	-0.28	-0.09	0.08	0.17	0.27	0.10	-0.50	0.57	0.76
		STD	0.53	0.49	0.45	0.36	0.30	0.16	0.05	0.07	0.26	0.43	0.52	0.62	0.45			
		RMS	1.41	1.68	1.75	1.64	1.69	1.44	1.20	0.88	0.30	0.30	0.73	1.25	0.67			
		χ^2	10.31	8.97	6.82	4.09	3.14	1.51	0.79	0.34	0.03	0.02	0.10	0.26	0.06			
	SAM	ε(P)	-0.89	-0.88	-0.87	-0.84	-0.81	-0.72	-0.65	-0.59	-0.51	-0.45	-0.35	-0.25	0.04	-0.87	0.51	1.01
		STD	0.29	0.28	0.27	0.24	0.22	0.12	0.05	0.01	0.09	0.15	0.24	0.35	0.64			
		RMS	1.42	1.75	1.90	1.93	2.12	2.01	1.94	1.82	1.73	1.76	1.56	1.17	0.29			
		χ^2	11.44	12.40	12.22	10.19	9.31	5.16	3.58	2.58	1.78	1.44	0.86	0.38	0.01			
	Proposed Method	ε(P)	0.01	-0.08	-0.11	-0.08	-0.10	0.00	0.04	0.08	0.09	0.04	0.02	0.03	-0.05	-0.01	0.05	0.05
		STD	0.02	0.07	0.10	0.07	0.09	0.01	0.05	0.09	0.09	0.05	0.03	0.04	0.04			
		RMS	0.02	0.16	0.24	0.18	0.26	0.00	0.12	0.25	0.29	0.14	0.08	0.15	0.36			
		χ^2	0.00	0.01	0.03	0.02	0.03	0.00	0.00	0.02	0.02	0.00	0.00	0.00	0.02			
May	ITU-R P. 618-13	ε(P)	-0.83	-0.76	-0.71	-0.65	-0.51	-0.36	-0.23	-0.13	0.07	0.29	0.42	0.52	0.64	-0.30	0.57	0.64
		STD	0.66	0.59	0.53	0.47	0.34	0.19	0.06	0.05	0.24	0.46	0.59	0.69	0.81			
		RMS	1.66	1.76	1.83	1.81	1.59	1.26	0.87	0.52	0.33	1.46	2.35	3.14	4.41			
		χ^2	8.25	5.67	4.40	3.29	1.66	0.71	0.26	0.07	0.02	0.33	0.69	1.08	1.72			
	SAM	ε(P)	-0.77	-0.77	-0.76	-0.76	-0.76	-0.60	-0.49	-0.44	-0.35	-0.27	-0.23	-0.17	-0.05	-0.64	0.39	0.75
		STD	0.28	0.27	0.26	0.26	0.27	0.11	0.00	0.05	0.14	0.22	0.27	0.32	0.45			
		RMS	1.54	1.77	1.97	2.12	2.36	2.10	1.86	1.82	1.62	1.38	1.28	1.02	0.31			
		χ^2	5.18	5.85	6.16	6.55	7.60	3.17	1.79	1.46	0.88	0.51	0.38	0.21	0.01			
	Proposed Method	ε(P)	0.10	0.02	-0.03	-0.07	-0.14	0.00	0.05	0.04	0.04	0.03	0.00	-0.01	-0.03	0.00	0.05	0.05
		STD	0.10	0.02	0.03	0.07	0.14	0.00	0.05	0.04	0.04	0.03	0.00	0.01	0.03			
		RMS	0.21	0.05	0.08	0.20	0.42	0.01	0.20	0.18	0.18	0.14	0.03	0.09	0.18			
		χ^2	0.02	0.00	0.00	0.02	0.07	0.00	0.01	0.01	0.01	0.00	0.00	0.00	0.01			

Table 7. Percentage error obtained over the interval [0.001% to 1%] for summer season.

Months	Methods	Parameters	Time Percentage (% p)													ITU-R P.311-15		
			1	0.5	0.3	0.2	0.1	0.05	0.03	0.02	0.01	0.005	0.003	0.002	0.001	μ_v	σ_v	ρ_v
June	ITU-R P. 618-13	ε(P)	-0.83	-0.77	-0.72	-0.67	-0.57	-0.50	-0.45	-0.40	-0.32	-0.21	-0.15	-0.10	-0.12	-0.58	0.38	0.70
		STD	0.38	0.32	0.27	0.22	0.13	0.05	0.00	0.05	0.13	0.23	0.29	0.35	0.33			
		RMS	1.83	2.00	2.15	2.20	2.23	2.44	2.59	2.58	2.52	1.95	1.56	1.08	1.66			
		χ^2	8.93	6.60	5.47	4.42	2.98	2.41	2.08	1.69	1.18	0.53	0.28	0.12	0.22			
	SAM	ε(P)	-0.97	-0.94	-0.72	-0.70	-0.74	-0.77	-0.73	-0.69	-0.58	-0.30	0.04	0.36	0.39	-0.92	0.85	1.26
		STD	0.49	0.46	0.23	0.21	0.25	0.28	0.24	0.20	0.09	0.19	0.53	0.84	0.88			
		RMS	2.14	2.46	2.17	2.30	2.87	3.77	4.23	4.49	4.55	2.71	0.45	3.91	5.38			
		χ^2	81.79	41.83	5.63	5.30	7.99	12.61	11.45	10.02	6.20	1.14	0.02	1.03	1.50			
	Proposed Method	ε(P)	-0.23	-0.11	0.41	0.36	0.17	-0.04	-0.10	-0.12	-0.14	-0.06	0.03	0.10	-0.04	0.00	0.14	0.14
		STD	0.25	0.12	0.39	0.35	0.15	0.06	0.11	0.14	0.16	0.07	0.01	0.08	0.06			
		RMS	0.51	0.27	1.23	1.20	0.65	0.21	0.55	0.78	1.10	0.51	0.34	1.06	0.54			
		χ^2	0.16	0.03	0.36	0.32	0.09	0.01	0.06	0.11	0.18	0.03	0.01	0.09	0.02			
July	ITU-R P. 618-13	ε(P)	-0.17	0.03	0.21	0.35	0.51	0.62	0.67	0.73	0.85	0.97	1.04	1.19	1.23	0.43	0.29	0.52
		STD	0.81	0.60	0.42	0.28	0.12	0.01	0.04	0.09	0.21	0.33	0.41	0.56	0.59			
		RMS	0.35	0.07	0.61	1.15	2.21	3.54	4.72	5.89	8.47	11.61	14.13	16.92	20.36			
		χ^2	0.07	0.00	0.11	0.30	0.75	1.36	1.90	2.48	3.88	5.71	7.20	9.20	11.22			
	SAM	ε(P)	-0.93	-0.79	-0.80	-0.63	-0.25	0.30	0.68	0.92	1.22	1.31	1.38	1.55	1.67	0.03	0.95	0.96
		STD	1.36	1.22	1.23	1.06	0.68	0.13	0.25	0.48	0.78	0.88	0.95	1.12	1.23			
		RMS	1.86	1.97	2.32	2.06	1.08	1.71	4.77	7.42	12.19	15.77	18.79	22.06	27.66			
		χ^2	23.89	7.24	9.21	3.44	0.36	0.40	1.93	3.55	6.70	8.95	10.90	13.43	17.28			
	Proposed Method	ε(P)	-0.48	-0.25	-0.33	-0.17	-0.02	0.10	0.13	0.12	0.09	0.01	-0.03	-0.02	-0.07	-0.07	0.17	0.18
		STD	0.41	0.18	0.26	0.10	0.05	0.17	0.20	0.19	0.16	0.08	0.04	0.05	0.00			
		RMS	0.97	0.63	0.95	0.56	0.07	0.58	0.93	1.01	0.89	0.18	0.45	0.29	1.24			
		χ^2	0.90	0.21	0.46	0.11	0.00	0.05	0.11	0.11	0.07	0.00	0.02	0.01	0.10			
August	ITU-R P. 618-13	ε(P)	-0.53	-0.41	-0.30	-0.19	-0.04	0.12	0.21	0.32	0.47	0.56	0.64	0.71	0.82	0.12	0.36	0.38
		STD	0.71	0.59	0.48	0.37	0.23	0.06	0.03	0.14	0.28	0.37	0.46	0.53	0.64			
		RMS	1.00	0.98	0.84	0.59	0.17	0.58	1.21	2.02	3.56	5.19	6.72	8.10	10.63			
		χ^2	1.11	0.67	0.36	0.14	0.01	0.06	0.21	0.49	1.13	1.86	2.62	3.37	4.80			
	SAM	ε(P)	-0.83	-0.78	-0.78	-0.78	-0.80	-0.59	-0.45	-0.31	0.26	1.46	2.36	2.86	3.15	-0.21	1.04	1.06
		STD	1.20	1.14	1.14	1.15	1.17	0.96	0.82	0.68	0.10	1.09	2.00	2.49	2.79			
		RMS	1.58	1.87	2.18	2.43	3.12	2.84	2.57	1.97	2.00	13.58	24.82	32.61	40.67			
		χ^2	7.87	6.53	7.57	8.75	12.56	4.10	2.12	0.89	0.41	8.06	17.44	24.16	30.88			
	Proposed Method	ε(P)	0. 43	0.30	0.17	0.08	-0.11	-0.07	-0.11	-0.12	-0.06	0.02	0.05	0.04	-0.02	0.02	0.11	0.12
		STD	0.39	0.26	0.12	0.03	0.16	0.12	0.16	0.17	0.11	0.02	0.00	0.01	0.07			
		RMS	0.82	0.73	0.47	0.23	0.44	0.35	0.65	0.78	0.47	0.23	0.51	0.43	0.28			
		χ^2	0.25	0.17	0.07	0.02	0.05	0.03	0.08	0.11	0.03	0.01	0.02	0.02	0.01			

Table 8. Percentage error obtained over the interval [0.001% to 1%] for fall season.

Months	Methods	Parameters	Time Percentage (% p)													ITU-R P.311-15		
			1	0.5	0.3	0.2	0.1	0.05	0.03	0.02	0.01	0.005	0.003	0.002	0.001	μ_v	σ_v	ρ_v
September	ITU-R P. 618-13	ε(P)	-0.63	-0.53	-0.43	-0.33	-0.13	0.12	0.25	0.37	0.53	0.71	0.69	0.75	0.84	0.07	0.43	0.43
		STD	0.80	0.70	0.60	0.50	0.30	0.06	0.08	0.20	0.36	0.54	0.52	0.58	0.67			
		RMS	1.01	1.06	0.99	0.82	0.38	0.38	0.96	1.57	2.73	4.28	5.01	6.04	7.83			
		χ^2	1.75	1.20	0.76	0.40	0.06	0.04	0.19	0.43	0.95	1.78	2.04	2.60	3.58			
	SAM	ε(P)	-0.67	-0.70	-0.69	-0.69	-0.70	-0.48	-0.34	-0.20	0.09	0.64	1.07	1.47	1.75	-0.18	0.69	0.71
		STD	0.71	0.74	0.73	0.73	0.74	0.53	0.38	0.25	0.04	0.60	1.03	1.43	1.71			
		RMS	1.07	1.39	1.58	1.71	2.03	1.60	1.29	0.86	0.44	3.83	7.84	11.76	16.31			
		χ^2	2.13	3.18	3.51	3.74	4.74	1.50	0.66	0.22	0.03	1.49	4.06	7.00	10.39			
	Proposed Method	ε(P)	0.33	0.11	0.03	-0.02	-0.13	-0.03	-0.03	-0.03	-0.04	0.03	0.01	0.03	-0.02	0.01	0.07	0.07
		STD	0.31	0.10	0.01	0.04	0.15	0.05	0.05	0.05	0.06	0.01	0.01	0.01	0.03			
		RMS	0.53	0.23	0.06	0.06	0.37	0.10	0.12	0.14	0.23	0.18	0.07	0.22	0.16			
		χ^2	0.13	0.02	0.00	0.00	0.05	0.00	0.00	0.00	0.01	0.01	0.00	0.01	0.00			
October	ITU-R P. 618-13	ε(P)	-0.82	-0.76	-0.70	-0.63	-0.50	-0.34	-0.20	-0.08	0.13	0.29	0.33	0.34	0.31	-0.29	0.50	0.57
		STD	0.62	0.56	0.50	0.42	0.30	0.14	0.01	0.12	0.33	0.49	0.54	0.54	0.51			
		RMS	1.15	1.29	1.33	1.25	1.15	0.89	0.55	0.23	0.43	1.15	1.57	1.84	2.13			
		χ^2	5.35	4.14	3.07	2.10	1.15	0.46	0.13	0.02	0.05	0.26	0.39	0.47	0.50			
	SAM	ε(P)	-0.73	-0.75	-0.75	-0.73	-0.75	-0.76	-0.60	-0.51	-0.36	-0.11	0.16	0.25	0.56	-0.53	0.51	0.74
		STD	0.34	0.36	0.36	0.34	0.36	0.36	0.21	0.12	0.03	0.28	0.55	0.64	0.95			
		RMS	1.03	1.28	1.43	1.47	1.72	1.97	1.69	1.54	1.23	0.45	0.76	1.32	3.89			
		χ^2	2.84	3.89	4.28	4.03	5.07	6.11	2.57	1.63	0.69	0.06	0.11	0.26	1.40			
	Proposed Method	ε(P)	0.25	0.08	0.01	0.01	-0.09	-0.17	-0.05	-0.01	0.02	0.04	0.05	0.00	-0.03	0.00	0.07	0.07
		STD	0.24	0.07	0.00	0.00	0.10	0.18	0.05	0.02	0.01	0.04	0.04	0.00	0.04			
		RMS	0.35	0.14	0.02	0.01	0.22	0.45	0.13	0.03	0.06	0.18	0.24	0.02	0.22			
		χ^2	0.07	0.01	0.00	0.00	0.02	0.09	0.01	0.00	0.00	0.01	0.01	0.00	0.01			
November	ITU-R P. 618-13	ε(P)	-0.79	-0.72	-0.69	-0.67	-0.68	-0.53	-0.46	-0.35	-0.17	0.03	0.19	0.24	0.47	-0.41	0.46	0.61
		STD	0.48	0.40	0.37	0.36	0.36	0.22	0.14	0.03	0.15	0.34	0.51	0.56	0.79			
		RMS	0.87	0.93	1.18	1.42	2.26	1.81	1.79	1.36	0.74	0.12	0.95	1.32	2.69			
		χ^2	3.39	2.35	2.65	2.94	4.84	2.08	1.54	0.73	0.15	0.00	0.15	0.26	0.86			
	SAM	ε(P)	-0.61	-0.65	-0.69	-0.74	-0.82	-0.72	-0.68	-0.62	-0.54	-0.47	-0.39	-0.32	0.00	-0.71	0.33	0.78
		STD	0.06	0.09	0.13	0.18	0.26	0.16	0.12	0.06	0.02	0.09	0.16	0.23	0.56			
		RMS	0.67	0.85	1.17	1.54	2.70	2.43	2.62	2.42	2.31	2.17	1.92	1.74	0.00			
		χ^2	1.07	1.58	2.55	4.30	11.98	6.21	5.55	3.94	2.71	1.91	1.24	0.83	0.00			
	Proposed Method	ε(P)	0.89	0.64	0.35	0.11	-0.27	-0.13	-0.15	-0.09	-0.06	-0.05	-0.02	-0.03	0.12	0.03	0.18	0.18
		STD	0.79	0.54	0.25	0.01	0.37	0.23	0.25	0.19	0.16	0.15	0.12	0.13	0.01			
		RMS	0.98	0.83	0.59	0.23	0.89	0.44	0.57	0.35	0.26	0.22	0.09	0.16	0.66			
		χ^2	0.46	0.33	0.15	0.02	0.32	0.07	0.10	0.03	0.02	0.01	0.00	0.01	0.07			

In addition, frequency scaling approach is tested for monthly variation of rain attenuation in Ka-band along the same and different communication paths. Frequency scaling method provides an alternative to rain attenuation models which are considered excellent predictors and provide a means for determining what to expect at a frequency for which there are no data. The mathematical expression for the determination of long term frequency scaling of rain attenuation statistics are listed in Equations (6a), (6b), (6c).

$$A_2 = A_1 \left(\frac{\varphi_2}{\varphi_1}\right)^{1-H(\varphi_1,\varphi_2,A_1)} \tag{6a}$$

where,

$$\emptyset(f) = \frac{f^2}{1+10^{-4}f^2} \tag{6b}$$

$$H\left(\emptyset_1, \emptyset_2, A_1\right) = 1.12 \times 10^{-3} \left(\frac{\varphi_2}{\varphi_1}\right)^{0.5} \left(\emptyset_1 A_1\right)^{0.55} \tag{6c}$$

A_1 and A_2 are the equiprobable values of the rain attenuation at frequencies f_1 and f_2 (GHz), respectively [13].

The analyses performed for month wise estimation of rain attenuation for 19.8 and 20.73 GHz is depicted in Figures 9(a) and 9(b) for 2013 year only because of good arrangement of data measurement in this year as compared to other years. These show that the estimations for 19.8 and 20.73 GHz are relatively higher than the measured values. For instance, the calculated rain attenuation values at 19.8 and 20.73 GHz links are 6.1, 8.5, 11.0 dB; 12.2, 15.5, 18.0 dB; 9.6, 14.3, 19.6 dB; 7.1, 11.2, 16.3 dB and 6.6, 11.0, 11.8 dB; 11.8, 15.7, 22.9 dB; 9.7, 16.3, 19.3 dB; 6.9, 11.2, 17.5 dB respectively at 0.1%, 0.01%, 0.001% of the time. The estimated values are 20.4, 23.9, 28.5 dB; 24.6, 33.4, 42.5 dB; 21.3, 28.9, 33.4 dB; 20.2, 25.5, 27.6 dB and 21.9, 25.8, 30.7 dB; 26.5, 35.9, 45.5 dB; 22.9, 31.1, 35.9 dB; 21.7, 27.4, 29.7 dB.

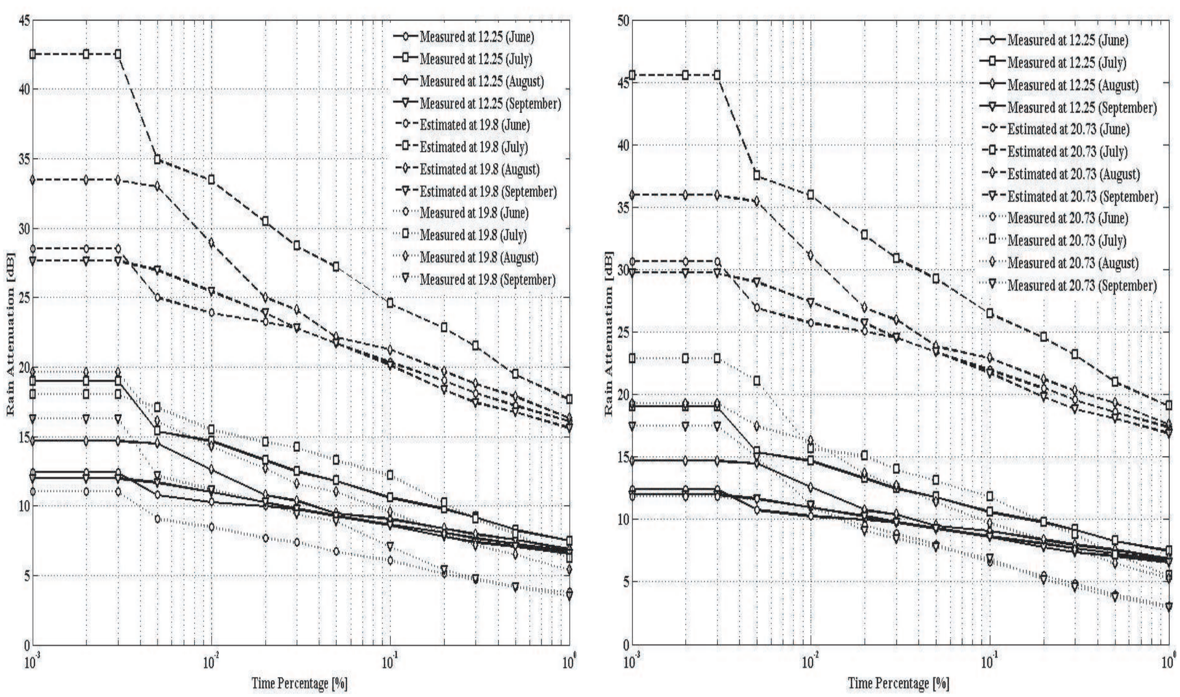

(a) (b)

Figure 9. (a) Cumulative distribution of rain attenuation obtained for 2013 year after frequency scaling in 19.8 GHz [24]. (b) Cumulative distribution of rain attenuation obtained for 2013 year after frequency scaling in 20.73 GHz [24].

5. CONCLUSIONS

The diurnal and monthly variations of slant path rain attenuation are presented for Mokdong Station in South Korea. The corresponding effective path length is calculated with the application of Simple Attenuation Model at 19.8 GHz for COMS1 satellite. It is obtained that higher fade margin is needed for reliable link availability, and the rain attenuation probability is lower in late night time and higher in morning hours. The rain attenuation and rain rate, collected over four years during 2013–2016 in the 12.25 and 20.73 GHz from Koreasat 6 and 19.8 GHz from COMS1 for Mokdong Station, were analyzed on monthly basis to observe the statistical characteristics. As first approach to this open research problem, a statistical analysis has been proposed to predict the time series of rain attenuation, effective path length and specific attenuation at Ka band over an earth space path. It has been found that the empirically derived k and α values provide data very close to the measured attenuation and can be sufficiently used to estimate rain attenuation in this region for all time percentages when $0.001\% \leq P \leq 1\%$ of the time. Further, the predictive capabilities of the models are judged through the relative error analyses, standard deviation, root mean square and chi-square values as well as through the recommendation of ITU-R P. 311-15 method. Thus, the paper presents the comparison of the measured data with the existing ITU-R rain attenuation prediction model for slant path communication and shows suitable approach for the categorization of best fitting approach. However, it should be noted that the results are valid for these particular climates, and its feasibility for other regions requires more testing and analyses.

All in all, we can adopt ITU-R P. 618-13 rain attenuation model in South Korea for better prediction of rain attenuation until the sufficient database of rain attenuation and rain rate from other locations become available. In addition, a frequency scaling scheme is analyzed as per the recommendation of ITU-R P. 618-13. These analyses shall be helpful to system designer for selecting suitable time margin for high data rate communication with higher link availability so as to maintain lower fade margin and for further enhancement of rain compensation methods.

Conflict of Interests

The authors declare that there is no conflict of interests regarding the publication of this paper.

REFERENCES

1. Lekkla, R. and P. Prapinmongkolkarn, "Diurnal variations in rain attenuation on Ku band earth-space paths," *International Journal of Satellite Communications*, Vol. 16, No. 5, 219–236, 1998.
2. Ojo, J. S. and O. C. Rotimi, "Diurnal and seasonal variations of rain rate and rain attenuation on Ku-band satellite systems in a tropical region: A synthetic storm techniques approach," *Journal of Computer and Communications*, Vol. 3, No. 4, 1, 2015.
3. Allnutt, J. E. and F. Haidara, "Ku-band diurnal fade characteristics and fade event duration data from three, two-year, Earth-space radiometric experiments in Equatorial Africa," *International Journal of Satellite Communications*, Vol. 18, No. 3, 161–183, 2000.
4. Elbert, B. R., *Introduction to Satellite Communication*, Artech House, 2008.
5. Konefal, T., et al., "Prediction of monthly and annual availabilities on 10–50 GHz satellite-Earth and aircraft-to-aircraft links," *IEE Proceedings — Microwaves, Antennas and Propagation*, Vol. 147, No. 2, 122–127, 2000.
6. Matricciani, E., "Diurnal distribution of rain attenuation in communication and broadcasting satellite systems at 11.6 GHz in Italy," *IEEE Transactions on Broadcasting*, Vol. 44, No. 2, 250–258, 1998.
7. Riva, C., "Seasonal and diurnal variations of total attenuation measured with the ITALSAT satellite at Spino d'Adda at 18.7, 39.6 and 49.5 GHz," *International Journal of Satellite Communications and Networking*, Vol. 22, No. 4, 449–476, 2004.
8. Das, S., A. Maitra, and A. K. Shukla, "Diurnal variation of slant path Ka-band rain attenuation at four tropical locations in India," *Indian Journal of Radio and Space Physics*, Vol. 42, No. 1, 34–41, 2013.

9. Ippolito, L. J., Jr., *Satellite Communications Systems Engineering: Atmospheric Effects, Satellite Link Design and System Performance*, Vol. 6, John Wiley & Sons, 2008.
10. Timothy, P., W. C. Bostian, and J. E. Allnutt, *Satellite Communication*, 2nd Edition, John Wiley & Sons, 2003.
11. Ojo, J. S., M. O. Ajewole, and S. K. Sarkar, "Rain rate and rain attenuation prediction for satellite communication in Ku and Ka bands over Nigeria," *Progress In Electromagnetics Research B*, Vol. 5, 207–223, 2008.
12. Singh, M. and J. E. Allnutt, "Rain attenuation predictions at Ku-band in South East Asia countries," *Progress In Electromagnetics Research*, Vol. 76, 65–74, 2007.
13. ITU-R P. 618-13, "Propagation data and prediction methods required for the design of Earth-space telecommunication systems," Geneva, Switzerland, 2017.
14. Sujan, S., J.-J. Park, and D.-Y. Choi, "Rain rate modeling of 1-min from various integration times in South Korea," *Springer Plus*, Vol. 5, No. 1, 2016.
15. Shrestha, S., J.-J. Park, S. W. Kim, J. J. Kim, J. H. Jung, and D. Y. Choi, "1-minute rain rate derivation from various integration times in South Korea," *Korean Institute of Next Generation Computing*, Bangkok, Thailand, Jan. 2016.
16. Choi, D. Y., "Rain attenuation prediction model by using the 1-hour rain rate without 1-minute rain rate conversion," *Int. J. of Comput. Sci. Netw. Secur*, Vol. 6, 130–133, 2006.
17. Choi, D. Y., et al., "Comparison of measured rain attenuation in the 12.25 GHz band with predictions by the ITU-R model," *International Journal of Antennas and Propagation*, Vol. 2012, 2011.
18. Shrestha, S. and D.-Y. Choi, "Study of rain attenuation in Ka band for satellite communication in South Korea," *Journal of Atmospheric and Solar-Terrestrial Physics*, 2016.
19. ITU-R, "Specific attenuation model for rain for use in prediction methods," Recommendation P.838-3, ITU-R Recommendations, P Series, ITU, International Telecommunications Union, Geneva, 2005.
20. Zhao, Z.-W., M.-G. Zhang, and Z.-S. Wu, "Analytic specific attenuation model for rain for use in prediction methods," *International Journal of Infrared and Millimeter Waves*, Vol. 22, No. 1, 113–120, 2001.
21. ITU-R, "Rain height model for prediction methods," Recommendation P.839-4, ITU-R Recommendations, P Series, International Telecommunications Union, Geneva, 2013.
22. Stutzman, W. L. and K. M. Yon, "A simple rain attenuation model for Earth-space radio links operating at 10–35 GHz," *Radio Sci.*, Vol. 21, No. 1, 65–75, 1986.
23. National Radio Research Agency (RRA) 767, Bitgaram-ro, Naju-si, Jeollanam-do 58217, Republic of Korea, http://www.rra.go.kr/en/index.jsp.
24. www.mathworks.com, the mathworks, Inc. Protected by U.S. and international patents.
25. ITU-R P. 311-15, "Acquisition, presentation and analysis of data in studies of radiowave propagation," International Telecommunication Union, Geneva, 2013.
26. Downie, N. M. N. M. and R. W. Heath, *Basic Statistical Methods*, No. 4, HA29, D6, 1983.
27. Shrestha, S. and D.-Y. Choi, "Rain attenuation statistics over millimeter wave bands in South Korea," *Journal of Atmospheric and Solar-Terrestrial Physics*, Vol. 152–153, 2017.
28. Shrestha, S. and D.-Y. Choi, "Proposed one-minute rain rate conversion method for microwave applications in South Korea" *Journal of Information and Communication Convergence Engineering*, Vol. 14, No. 3, doi:10.6109/jicce.2016.14.3.153, Aug. 2016.
29. Shrestha, S. and D.-Y. Choi, "Characterization of rain specific attenuation and frequency scaling method for satellite communication in South Korea," *International Journal of Antennas and Propagation*, Vol. 2017, 2017.
30. Shrestha, S. and D.-Y. Choi, "Study of 1-min rain rate integration statistic in South Korea," *Journal of Atmospheric and Solar-Terrestrial Physics*, Vol. 155, 1–11, 2017.
31. Garcia-Rubia, J. M., et al., "Experimental assessment of slant-path rain attenuation variability in the Ka-band," *International Journal of Satellite Communications and Networking*, Vol. 34, No. 2,

155–170, 2016.

32. Allnutt, J. E. and F. Haidara, "Ku-band diurnal fade characteristics and fade event duration data from three, two-year, Earth-space radiometric experiments in Equatorial Africa," *International Journal of Satellite Communications and Networking*, Vol. 18, No. 3, 161–183, 2000.
33. Fiebig, U.-C. and C. Riva, "Impact of seasonal and diurnal variations on satellite system design in V band," *IEEE Transactions on Antennas and Propagation*, Vol. 52, No. 4, 923–932, 2004.
34. Boulanger, X., et al., "Four years of total attenuation statistics of earth-space propagation experiments at Ka-band in Toulouse," *IEEE Transactions on Antennas and Propagation*, Vol. 63, No. 5, 2203–2214, 2015.
35. Series, ITU Radiowave Propagation, "Characteristics of precipitation for propagation modelling," Recommendation ITU-R, 837-7, 2017.